مجله انجمن زمین‌شناسی مهندسی ایران
پاییز ۱۴۰۲، جلد شانزدهم، شماره ۳ صفحه ۱۳۱ تا ۱۴۸

Evaluating the cutting rate of travertine stones based on physico-mechanical characteristics through regression models

Amin Jamshidi[1*], Seyed Najmedin Almasi[2]

Received: 13.12.1401 Acepted: 25.08.1402

Abstract

Evaluating the cutting rate (*CR*) of stones is important in the cost estimation and the planning of the stone processing plants. This research used regression models to estimate the stones' *CR* based on their physico-mechanical characteristics. Stone processing factories in Mahallat City (Markazi province, Iran) were visited, and the *CR* of diamond circular saws was recorded on six different travertine stones. Next, the stone block samples were collected from the quarries for laboratory tests. Stones' porosity (*n*), uniaxial compressive strength (*UCS*), and Schmidt hammer hardness (*SH*) were determined in the laboratory as their physico-mechanical characteristics. Correlation relationships of *CR* with physico-mechanical characteristics were evaluated using simple and multiple regression analyses, and estimator models were developed. Results showed that multiple regression models are more reliable than simple regression for estimating the stones' *CR*. The validity of the developed multiple regression models was verified with the published data of one researcher. The findings indicated that these models are accurate enough for estimating the *CR* of stones. Consequently, the multiple regression models provide practical advantages for estimating the *CR* and save time and cost during the planning and design of the stone processing factories.

Keywords: *Cutting rate; Porosity; Schmidt hammer hardness; Travertine stones; Uniaxial compressive strength*

[1] Associate Professor, Department of Geology, Lorestan University, Khoramabad, Iran
[2] Assistant Professor, Department of Mining Engineering, Lorestan University, Khoramabad, Iran
*Corresponding Author: jamshidi.am@lu.ac.ir

1. Introduction

Circular diamond saws have been widely used in stone processing plants. Evaluating the stone sawability is very important in the planning for the plants and their cost estimation. Stone sawability can be measured in terms of the cutting rate (*CR*), also called slab production or production rate. *CR* is the quantity of the area cut per unit of time expressed as m^2/h. In practice, this criterion is calculated using the following equation:

$$CR = \frac{L \times H}{t} \quad (1)$$

where *CR* is the cutting rate (m^2/h), *L* (m) and *H* (m) are the cutting length and height of the stone block work-piece, respectively, and *t* (h) is the cutting time of the stone block work-piece.

CR depends on non-controlled parameters related to stone characteristics and controlled parameters related to characteristics of cutting tools and equipment. In the same working conditions, the sawing process and its results are strongly affected by the petrographic and physico-mechanical characteristics of the stone. Several studies have reported the relationship between *CR* and physico-mechanical characteristics such as porosity (*n*), uniaxial compressive strength (*UCS*), and Schmidt hammer hardness (*SH*) (Table 1).

Burgess (1978) proposed a regression equation for estimating the *CR* based on mineralogical composition, grain size, abrasion resistance, and hardness. Using regression analyses, Gunaydin et al. (2004) investigated the relationships between *CR* and various brittleness indices. They concluded that the *CR* of carbonate stones can be estimated from their brittleness indices. Kahraman et al. (2004) estimated the carbonate stones *CR* from their shear strength parameters through an artificial neural network (ANN). Delgado et al. (2005) experimentally investigated the correlation between the granite *CR* and its hardness. In their research, *CR* was chosen as the sawability criterion, and the hardness was calculated from mineral Vickers hardness. Experimental results indicated that using Vickers hardness could provide more precise information in evaluating the stone *CR*. Kahraman et al. (2006) investigated the correlation between *CR* and n for carbonate rocks. The results showed a power equation between these parameters with a determination coefficient (R^2) of 0.73. Fener et al. (2007) recommended using simple regression analyses to predict the *CR* of carbonate stones based on strength characteristics and Los Angles abrasion loss. Ataei et al. (2012) evaluated the *CR* of a diamond wire saw based on stone characteristics using regression analyses. Mikaeil et al. (2013) used stone brittleness indices (*B*) as a parameter to estimate the *CR* of ornamental stones using simple regression equations. The results showed no significant correlation between the *CR* and B_1 (*UCS*/*BTS*) and B_2 ((*UCS-BTS)*/(*UCS+BTS)*). However, a reliable estimation was extracted for *CR* based on B_3 ((*UCS-BTS)/2*) as a brittleness index. Tumac (2016) revealed a very weak correlation between *CR* and *n* (R^2 = 0.15) for marble and limestone. Almasi et al. (2017a) investigated relationships between *CR* and index characteristics for 11 types of hard dimension stones. These researchers found that the Mohs hardness, grain size, and *UCS* are among the most important parameters for estimating the stone *CR*. Jamshidi (2019) proposed a new estimator parameter for evaluating the *CR* of ornamental stones. This parameter is based on the product of *UCS* and Mohs hardness. It was concluded that the new estimator parameter has good accuracy for estimating *CR*, making it a convenient tool for the rapid *CR* assessment of stones. The influence of the Cerchar hardness index of granite stone on the wear of diamond tools was investigated by Rajpurohit et al. (2020). The results showed a positive correlation between the Cerchar hardness index and tool wear.

According to the literature review, several works have estimated the stone *CR* from its index characteristics. In recent years,

researchers have shown interest in new methods to solve problems involved in stone processing, such as their *CR*. These approaches are based on genetic algorithms, support vector regression (Beiki et al., 2013; Ceryan, 2016), probabilistic and soft computing techniques such as artificial neural networks, regression trees (Yurdakul et al., 2014; Aydin et al., 2015; Armaghani et al., 2016; Singh et al., 2017), adaptive neuro-fuzzy inference systems, fuzzy inference systems, hybrid ANN and GA, hybrid ANN and imperialist competitive algorithm, and hybrid ANN and particle swarm optimization technique (Mishra and Basu, 2013; Mohamad et al., 2015; Madhubabu et al., 2016). Despite the advantages of these techniques, they also have some disadvantages, such as a "black box" nature, greater computational burden, proneness to over-fitting, and the empirical nature of model development. These approaches may not be practical for project engineers to set up/run neural networks and fuzzy models. A piece of special knowledge is also needed for these models. Accordingly, the development of models using simple and multiple regression analyses can be preferred instead of these types of models. Fener et al. (2007) and Kahraman and Gunaydin (2008) are among the researchers who studied simple and multiple regression analyses for evaluating the *CR* of stones. Fener et al. (2007) suggested some significant equations using the multiple regression analysis and concluded that selected models had the advantages of using the index tests. Kahraman and Gunaydin (2008) correlated the indentation hardness index values with the *CR* of eight carbonate stones. They reported that the R^2 values derived using the multiple regression models were generally higher than those obtained using the simple regression.

The *n*, *UCS*, and *SH* are increasingly used worldwide by geotechnical and mining engineers regarding their simplicity, rapidity, low cost in execution, and non-destructiveness. As the index parameters, these characteristics have been used by some researchers in the building stones industry for a quick assessment of the various stones *CR* (Fener et al., 2007; Guney, 2011; Tumac, 2015; Almasi et al., 2017a; Jamshidi, 2019).

The present study aimed to develop new simple and multiple regression models for estimating the *CR* of travertine stones using the *n*, *UCS*, and *SH*. These models provide more insight and add more information to the correlations between *CR* of travertine stones with their *n*, *UCS*, and *SH*.

Table 1. Some of the correlations between *CR* with *n*, *UCS*, and *SH*

References	Rock type	Equation	R^2
Kahraman et al. (2004)	Limestone, Travertine	$CR = 43.90\ e^{0.017UCS}$	0.07
		$CR = -0.141\ SH + 23.76$	0.02
Kahraman et al. (2006)	Carbonate Rocks	$CR = 13.22\ n^{0.144}$	0.73
Fener et al. (2007)	Travertine, Limestone	$CR = -5.22\ \mathrm{Ln}(UCS) + 38.23$	0.73
		$CR = -0.19\ SH + 24.2$	0.29
Guney (2011)	Marble	$CR = -1.5\ SH + 97.0$	0.06
Mikaeil et al. (2013a)	Granite, Marble, Travertine	$CR = 161.53\ UCS^{-0.68}$	0.97
Mikaeil et al. (2013b)	Granite, Marble, Travertine	$CR = -5.19\ \mathrm{Ln}(UCS) + 31.24$	0.97
Tumac (2016)	Marble, Limestone	$CR = 6.80\ n + 9.52$	0.15
		$CR = 43.90\ e^{0.017UCS}$	0.69
Almasi et al. (2017a)	Igneous Rocks	$CR = 2.66\ \mathrm{Ln}(UCS) + 15.11$	0.41
Almasi et al. (2017b)	Igneous Rocks	$CR = 13.22\ UCS^{-1.352}$	0.36
Jamshidi (2019)	Igneous Rocks	$CR = 12.07\ e^{-0.007UCS}$	0.88

2. Materials and methods

Regression analyses are among the most commonly accepted methods of investigating the empirical relationships between stone parameters, such as physico-mechanical characteristics. These analyses are amenable to "ceteris paribus" analysis because they allow researchers to explicitly control many other factors that simultaneously affect the dependent variables. Multiple regression models can accommodate many explanatory variables that may be correlated. Therefore, researchers can hope to infer causality in cases where simple regression analysis would be misleading.

The present study used simple and multiple regression analyses to estimate the *CR* of the different travertine samples using their *n*, *UCS*, and *SH*. To achieve the objectives of the present study, we made field visits to the travertine quarries in the Mahallat area (Markazi Province, Central Iran) (Fig. 1). Then, stone processing factories around of Mahallat area were visited, and the *CR* of large-diameter circular saws were measured on six different travertine types. During the cutting operation in the processing factory, the cutting time (*t*) of the travertine stone block was obtained. Based on the recorded time, and cutting length and height (*L* and *H*, respectively) of the stone block work-piece, *CR* (m^2/h) for each travertine type was calculated according to Eq. (1) presented in the "Introduction" section. The *CR* values of the samples are given in Table 2.

After this step, the block samples were collected from various travertine quarries for laboratory tests. These samples are marketed in construction industries as ornamental, cladding, and building stones. During the sampling, blocks with no bedding planes and fractures were selected to eliminate the effect of anisotropy on the measurement. It is noteworthy that travertines are notoriously variable and heterogeneous in their properties (e.g., physico-mechanical characteristics), depending on the nature of their texture and porous media. In this respect, the heterogeneity of the test results was reduced by collecting some samples with approximately cubic shapes from various workfaces of quarries. The travertines block samples of each quarry were macroscopically completely different from other quarries. In the sampling process, it was tried to select fresh block samples from the quarry workface to obtain accurate results. To this end, an eye lens (loupe) was used to inspect the samples.

After transferring the block samples to the Laboratory of Engineering Geology and Rock Mechanics, the specimens with standard shapes and sizes (ISRM, 1981) were prepared from them using a coring machine (Fig. 2a). Finally, some of the physico-mechanical characteristics of the samples such as density (ρ), *n*, *UCS*, and *SH* were determined.

Table 2. *CR* values of the samples

Rock code	*CR* value (m^2/h)
Travertine 1	15.1
Travertine 2	14.2
Travertine 3	14.6
Travertine 4	16.2
Travertine 5	15.0
Travertine 6	15.6

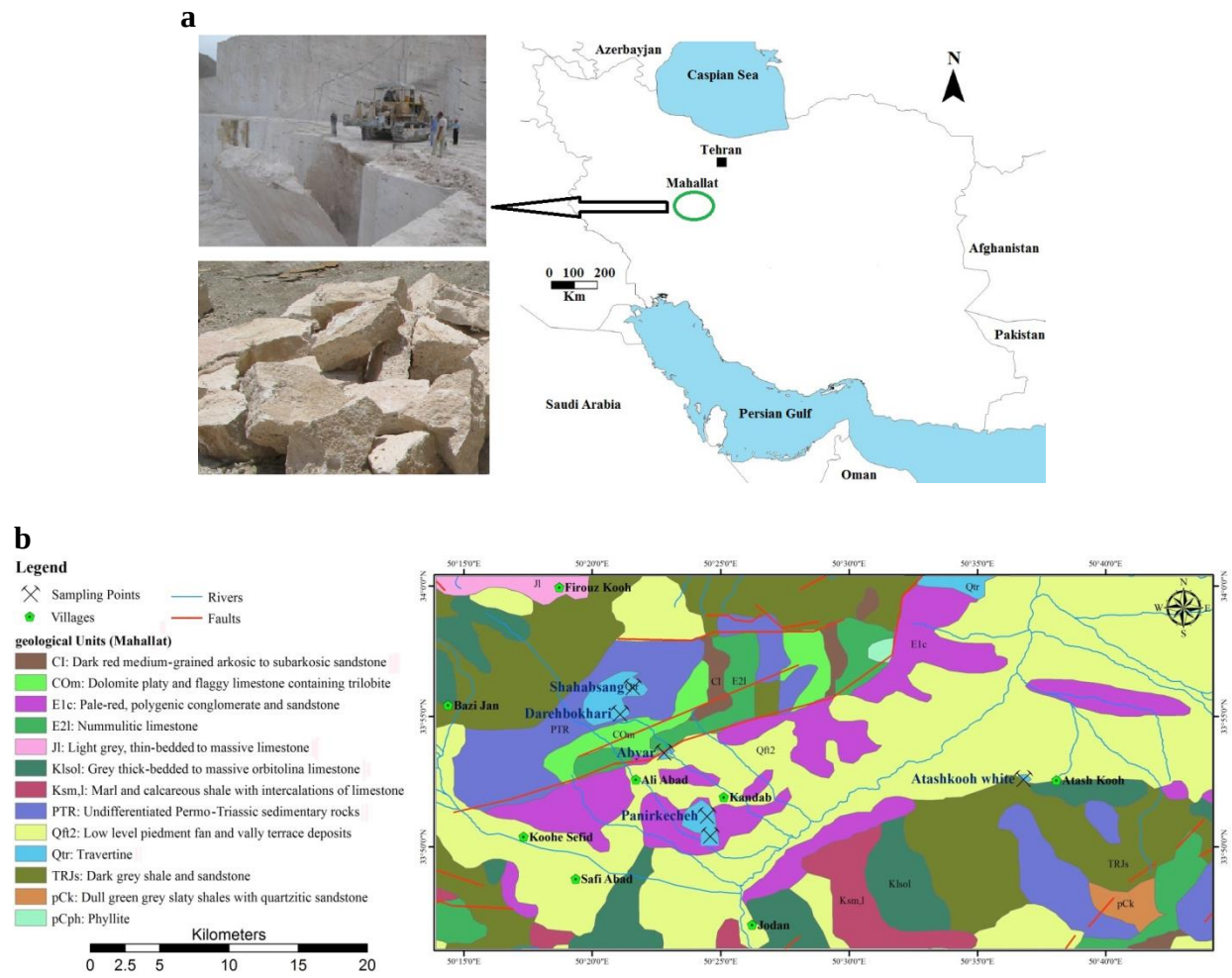

Figure 1. a) Sampling area on the map of Iran and some of the travertine blocks collected and **b)** sampling points on the geological map of the study area (after Zalooli et al., 2018)

2.1. Geological setting of the Mahallat area

The huge travertine reserves in Iran extend from the northwest to the southeastern across a long strip of 2000 km with an average width of 100 km and a very sharp trend. This strip, known as the "Urumieh Dokhtar Magmatic Belt" (UDMB), has numerous hot and volcanic springs and volcanic activities from the Pliocene to the present. The travertine samples obtained from the quarries in the Mahallat area are located in UDMB. In this belt, intense and intrusive magmatic activities occurred following the Laramide orogeny and declined gradually in some places after the Eocene. Extensive travertine deposits in the Mahallat area belong to the last phase of the volcanic activity of UDMB. The concentration of Mahallat travertines is in the UDMB. The intersection of magmatic zones with calcareous rocks in this area and the existence of underground waters heated by magmatic activities have led to the dissolution of these rocks. Soluble calcium and bicarbonate ions in underground waters reach the earth's surface through fractures, eventually forming travertine deposits in the Mahallat area (Bahrami et al., 2023).

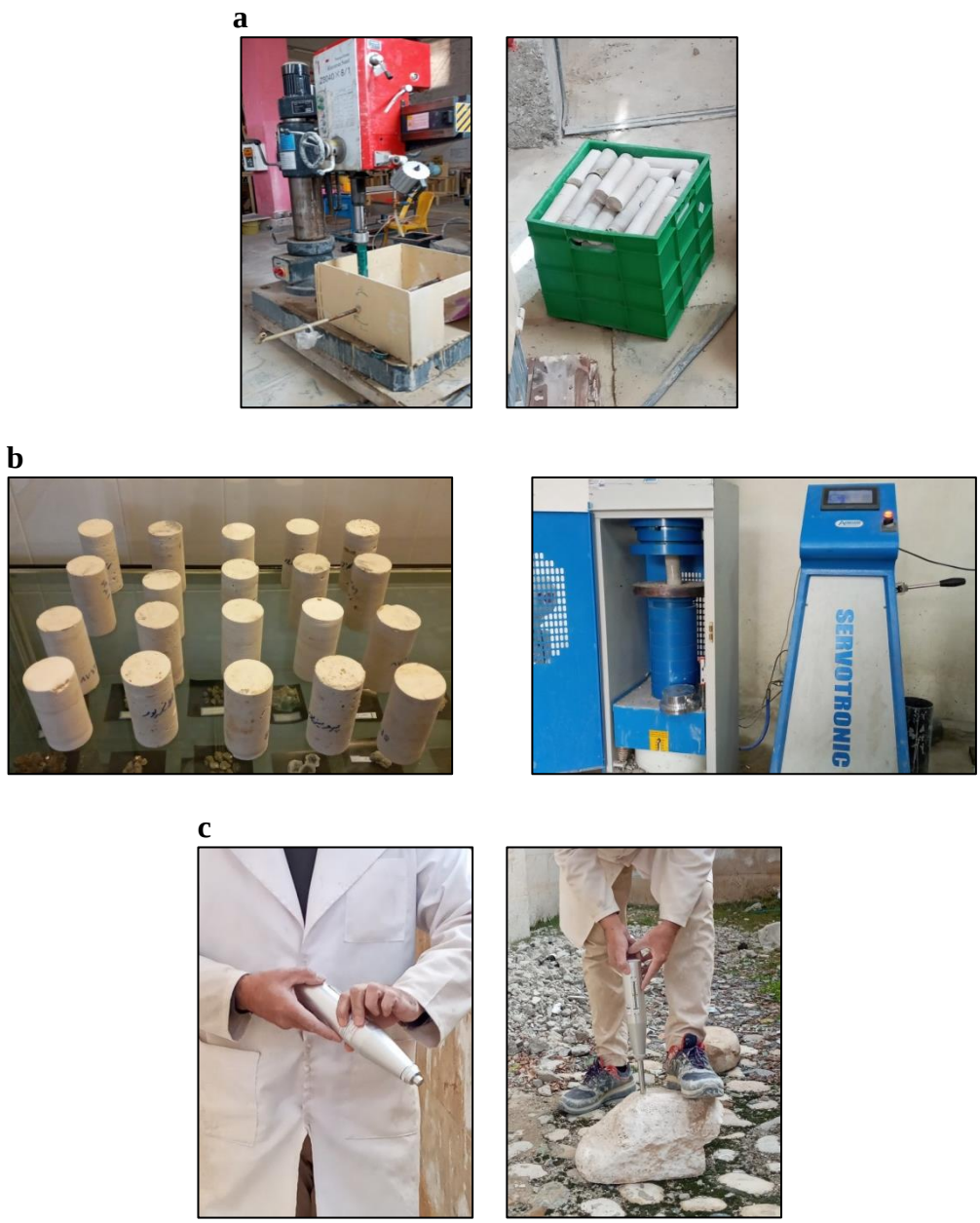

Figure. 2 a) The coring machine used in the present study and cylindrical core specimens prepared from travertine blocks, **b)** some of the core specimens and *UCS* device setup, and **c)** Schmidt hammer (N-type) device and performing test on the block sample

2.2. Morphology travertine deposits

The morphological features of the travertine deposits were investigated through several stages of field visits from the Mahallat quarries. From a morphological point of view, the area's travertine deposits can be categorized as a spring mound. The mound-type travertine deposits are formed on a pure carbonate substrate and are capped by stratified stromatolitic dolostones (Roshanak et al., 2018). In the study area, travertine mounds were observed up to a height of approximately 110 m.

Travertines can be categorized into thermogenic and meteogenic types based on the reactions leading to CO_2 release (Pentecost 2005). Travertines of the thermogenic type are often associated with

regions of recent volcanic or tectonic activity. High carbon isotope values up to 11% (VPDB; Vienna Pee Dee Belemnite) show that Mahallat travertines (samples studied in present research) have been deposited from thermal waters rich in deep-sourced heavy CO_2 released during the thermo-metamorphic decarbonization of carbonate-bearing bedrocks. Therefore, they belong to the travertine of thermogenic type (Zarasvandi et al., 2019).

2.3. Petrographic characteristics

The travertine samples were characterized by their petrographic characteristics using an optical polarizing microscope. To this end, specimen pieces were prepared from the travertine blocks and superficially impregnated using a fluorescence dye epoxy resin under vacuum pressure. Then, microscopic thin sections were obtained from each travertine type. For further specification of mineralogical composition, powder X-ray diffraction (XRD) analysis was carried out using an "STOE model" diffractometer. According to the thin-section examinations and XRD analyses (Fig. 3), calcite mineral is the studied samples' major constituent, with its crystals being in clusters and rhombohedral. The samples' structure is dominated by pores, many of which are in the form of non-connected. The pore space distribution was almost intense, and its geometry was frequently irregular. The samples' texture is a community of micrite and sparite. Furthermore, fabric-controlled pore space is observed as intergranular and shelter. The laboratory studies of Jamshidi et al. (2016) and Zalooli et al. (2018) indicated that the mechanical behavior of the travertine deposits of the Mahallat area, especially strength characteristics, is strongly influenced by their porous nature.

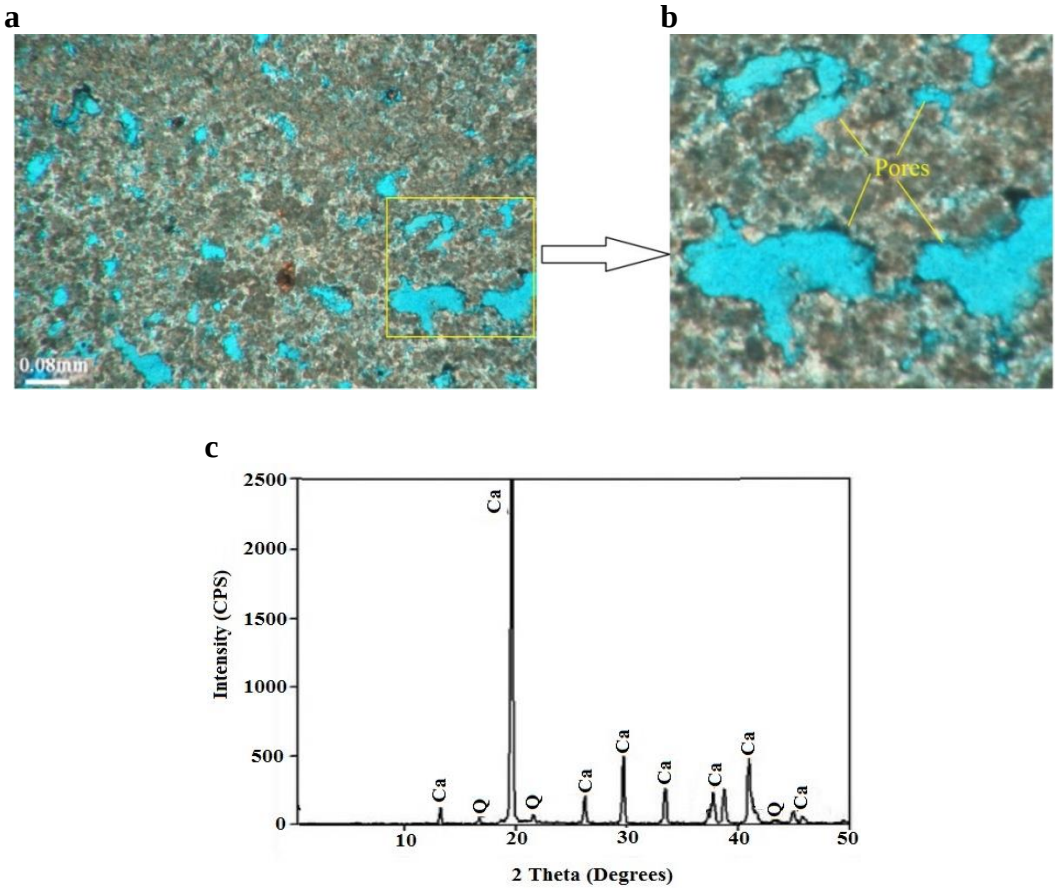

Figure 3. a) Image of the microscopic thin-section of the representative sample (Travertine 1) showing the intensity distribution and the irregular shape of pore space, **b)** A magnified view of the outlined region in (a), and **c)** Results of XRD analysis for representative

2.4. Physico-mechanical characteristics

Some of the physical characteristics of the samples, including ρ and n were determined following the recommendations of ISRM (1981). Five specimens in the form of cut blocks from each travertine type were used to determine ρ and n. The results are given in Tables 3 and 4. Based on the test results and using the method proposed by Anon (1979), the samples are categorized as stones with medium and high ρ (2.20-2.50 g/cm^3 and 2.50-2.70 g/cm^3, respectively), and medium and high n (5-15% and 15-30%, respectively) (Fig. 4).

Table 3. The determined results of ρ (g/cm^3) for travertine samples

Rock code	Number of tested specimens	Test standard/Specimen shape	Minimum	Maximum	Mean
Travertine 1	5	ISRM (1981)/Cut block	2.34	2.41	2.38
Travertine 2	5	ISRM (1981)/Cut block	2.39	2.47	2.44
Travertine 3	5	ISRM (1981)/Cut block	2.44	2.53	2.47
Travertine 4	5	ISRM (1981)/Cut block	2.41	2.53	2.48
Travertine 5	5	ISRM (1981)/Cut block	2.32	2.39	2.34
Travertine 6	5	ISRM (1981)/Cut block	2.47	2.56	2.53

Table 4. The determined results of n (%) for travertine samples

Rock code	Number of tested specimens	Test standard/Specimen shape	Minimum	Maximum	Mean
Travertine 1	5	ISRM (1981)/Cut block	11.6	13.3	12.8
Travertine 2	5	ISRM (1981)/Cut block	10.4	12.7	11.9
Travertine 3	5	ISRM (1981)/Cut block	13.8	15.5	14.3
Travertine 4	5	ISRM (1981)/Cut block	16.6	18.4	17.3
Travertine 5	5	ISRM (1981)/Cut block	14.6	16.7	15.5
Travertine 6	5	ISRM (1981)/Cut block	13.9	15.8	15.1

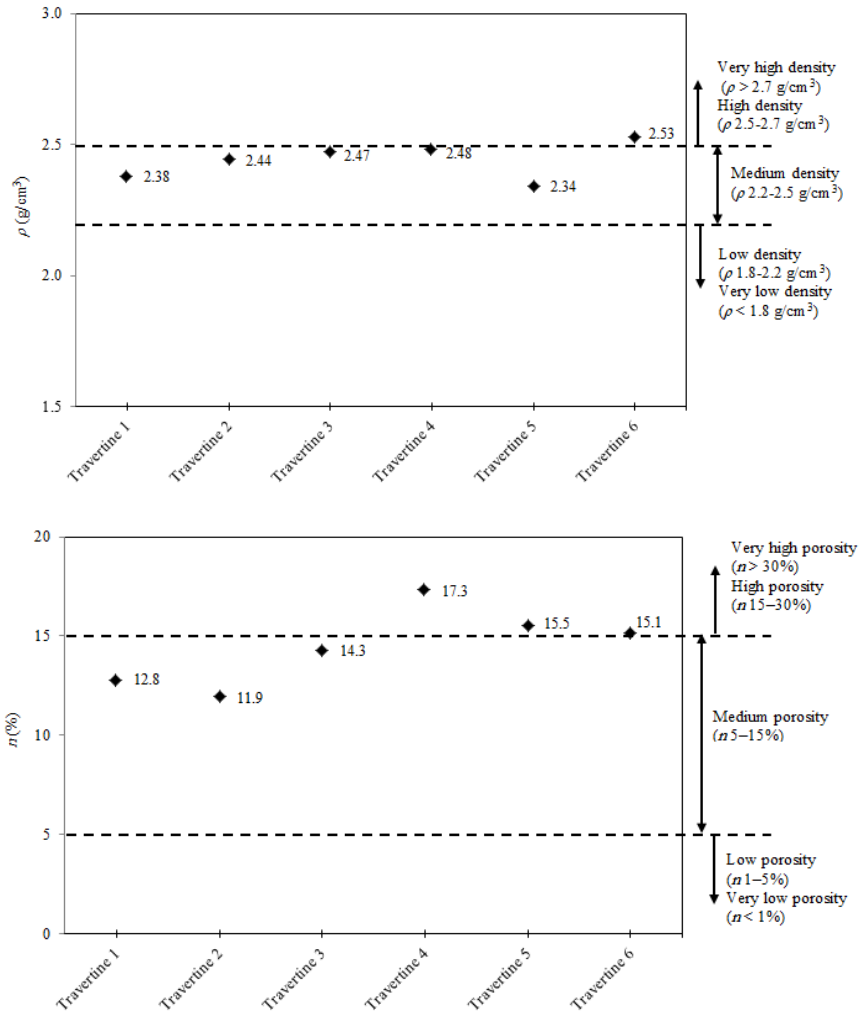

Figure 4. Classification of the samples based on their ρ and n (Anon, 1979)

Before performing the *UCS* tests, the core specimens were prepared from the block samples. Next, the edges of the specimens were cut parallel and smooth to provide in shape and size according to ISRM (1981) (Fig. 2b). For each travertine type, five specimens were tested, and mean values were calculated accordingly. The values of *UCS* for samples are given in Table 5. This table shows that the samples' *UCS* values are between 44.1 and 66.0 MPa. In addition, the studied samples are classified according to their *UCS* values, as suggested in ISRM (2007). According to Fig. 5, most samples were classified as rocks with medium strength (50-100 MPa), except travertines 4 and 5 that fall into the rocks class with low strength (25-50 MPa).

The *SH* test was performed with an N-type hammer having an impact energy of 2.207 Nm according to ISRM (1981). Tests were carried out on the block samples having an approximate dimension of 0.20 m × 0.40 m × 0.40 m. All tests were made with the hammer held vertically downward and at a right angle to the horizontal faces of the samples (Fig. 2c). It is of note that each block sample was inspected for macroscopic defects to eliminate any anisotropy effects on the measurement. The results of *SH* tests are presented in Table 6. Studied travertine samples are classified according to their *SH* values as suggested in ISRM (1978). Fig. 6 shows that samples concerning their *SH* values fall into the different stones class with slightly strong (*SH* = 20-40) and strong strength (*SH* = 40-50).

Table 5. *UCS* (MPa) values of the samples

Rock code	Number of tested specimens	Test standard/Specimen shape	Minimum	Maximum	Mean
Travertine 1	5	ISRM (1981)/Cylindrical core	49.1	56.4	52.2
Travertine 2	5	ISRM (1981)/Cylindrical core	62.4	69.0	65.1
Travertine 3	5	ISRM (1981)/Cylindrical core	63.7	69.9	66.0
Travertine 4	5	ISRM (1981)/Cylindrical core	40.3	46.2	44.1
Travertine 5	5	ISRM (1981)/Cylindrical core	45.8	52.1	48.7
Travertine 6	5	ISRM (1981)/Cylindrical core	46.6	55.7	51.1

Table 6. *SH* values of the samples

Rock code	Number of tested specimens	Test standard/Specimen shape	Minimum	Maximum	Mean
Travertine 1	3	ISRM (1981)/Block	34	42	37
Travertine 2	3	ISRM (1981)/Block	39	44	42
Travertine 3	3	ISRM (1981)/Block	42	48	46
Travertine 4	3	ISRM (1981)/Block	31	37	33
Travertine 5	3	ISRM (1981)/Block	35	39	36
Travertine 6	3	ISRM (1981)/Block	35	40	38

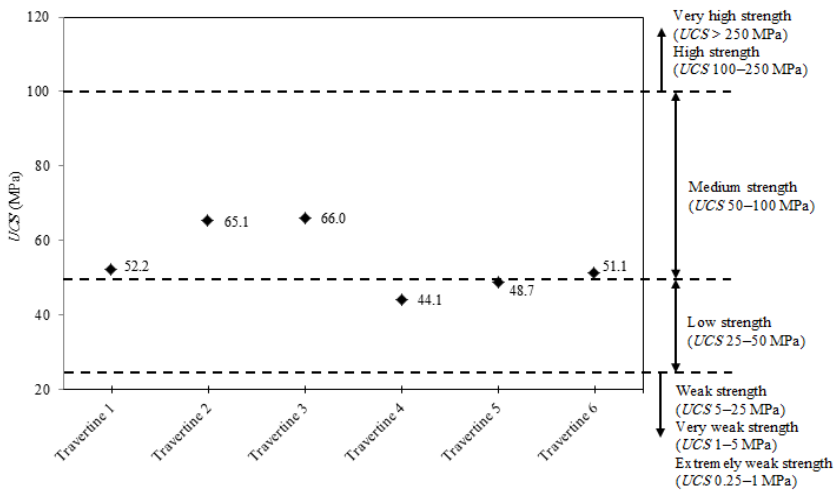

Figure 5. *UCS* classification of the samples (ISRM, 2007)

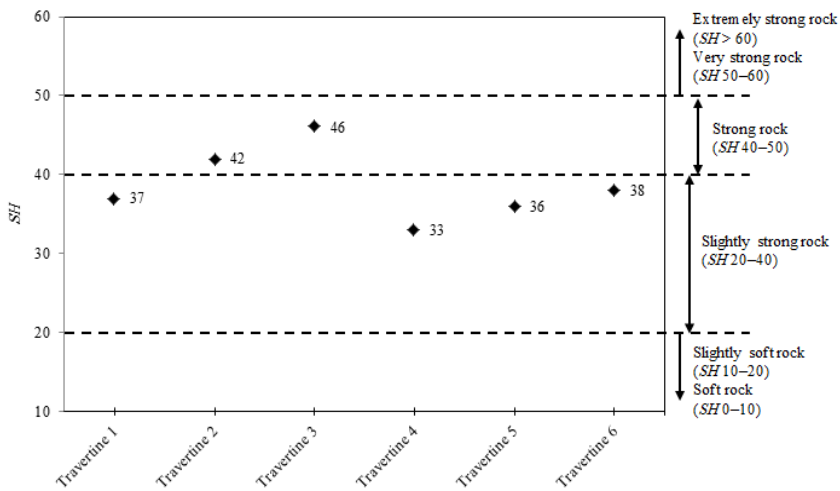

Figure 6. Classification of the samples based on their *SH* (ISRM, 1978)

3. Statistical analyses of the test results

Simple regression analyses, including linear ($y = ax + b$), power ($y = ax^b$), exponential ($y = ae^x$), and logarithmic ($y = a + \ln x$) regression, were conducted on the data presented in Tables 2 and 4-6 to investigate the correlations between *CR* with *n*, *UCS*, and *SH* of the samples. These analyses were performed to develop the best correlation between different variables to attain the most reliable empirical equation.

Fig. 7 presents the correlation between *CR* and *n* for the prepared samples. This figure indicates a moderate linear correlation between *CR* and *n* ($R^2 = 0.69$). The changes of *CR* as a function of *UCS* are depicted in Fig. 7. As can be seen, the best-fitted correlation was offered by a power regression curve. A moderate power correlation between *CR* and *UCS* was obtained with an R^2 of 0.79. Similarly, a power correlation was observed between *CR* and *SH* with a lower R^2 of 0.65.

According to Fig. 7, *CR* has a stronger correlation with *UCS* ($R^2 = 0.79$) compared with correlations between *CR* with n and *SH* (R^2 of 0.69 and 0.65, respectively). Besides, *CR* has a weaker correlation with *SH* than n and *UCS*. This difference can be attributed to the nature of the *SH* test on the stone block samples. The heterogeneity of the block sample surfaces is among the most important factors affecting the accuracy of the *SH* test. The studied samples in the present research are travertine stones, which are highly heterogeneous due to their porous nature. The heterogeneity of block sample surfaces will create scatters in the *SH* test results, leading to a weak correlation between *CR* and *SH*.

The literature reports some correlations to estimate the *CR* of stones using the *n*, *UCS*, and *SH*, which give the different relationships (linear and non-linear) (Table 1). As can be seen from Table 1, the derived correlations in this study have similarities and differences from the correlation equation and R^2 values available in the literature.

Multiple regression analyses were performed to investigate the relationships between *CR* with *n*, *UCS*, and *SH* of the samples. The dependent variable is the *CR*, and the independent variables are *n*, *UCS*, and *SH*. The regression analyses are performed using the SPSS®v.16 code statistical software. Multivariate regression analyses were conducted with a 95% confidence level and the best-fit curves were obtained using the least squares method. The best-fitting models obtained using the independent variables are as follows:

$$CR = 15.40 + 0.152\,n - 0.045\,UCS \quad R^2 = 0.84 \tag{2}$$

$$CR = 14.89 - 0.205\,n + 0.071\,SH \quad R^2 = 0.83 \tag{3}$$

$$CR = 17.63 - 0.123\,UCS + 0.108\,SH \quad R^2 = 0.80 \tag{4}$$

where *CR* (m^2/h) is the cutting rate and *n* (%), *UCS* (MPa), and *SH* are porosity, uniaxial compressive strength, and Schmidt hammer hardness, respectively.

The coefficient of determination (R^2) and standard error of estimate (*SEE*) were used as the numerical measures of the goodness of fitting curves for the regression equations. The degree of fit to a curve can be measured by R^2 and *SEE*. R^2 measures the proportion of variation in the dependent variable. On the other hand, *SEE* indicates how close the measured data points fall to the estimated values on the regression curve. The R^2 and *SEE* values of Eqs. (2-4) are given in Table 7. As can be seen from this table, the R^2 of Eqs. (2-4) are higher than 0.80, which is acceptable. The *SEE* values for these equations are 0.36, 0.38, and 0.41, respectively. These measures show that Eqs. (2-4) can be accepted as a highly reliable estimate for the *CR* using *n*, *UCS*, and *SH* using the coefficients in Table 7.

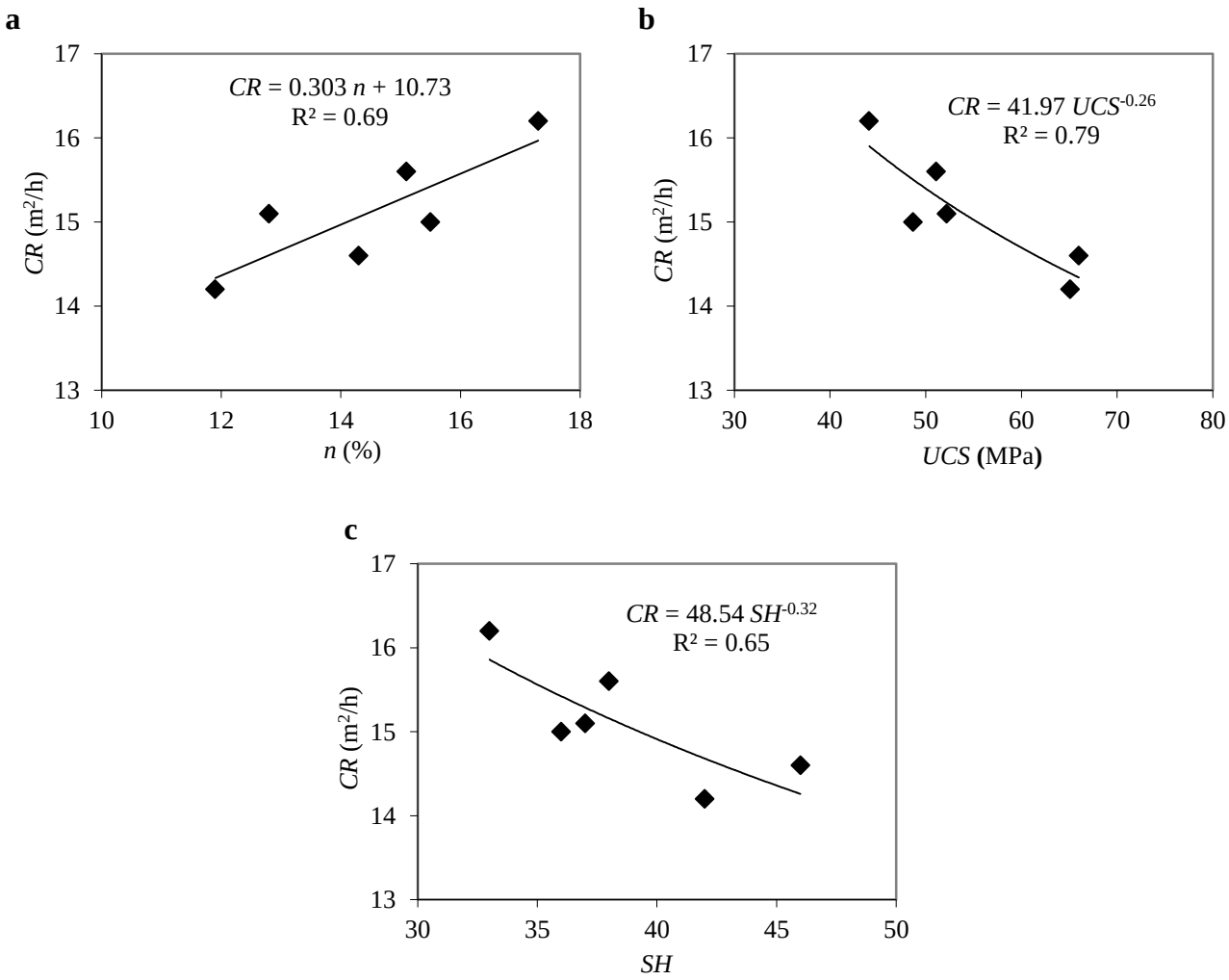

Figure 7. The correlations between *CR* and **a)** *n*, **b)** *UCS*, and **c)** *SH*

Table 7. Regression coefficients for estimating the *CR* of the samples using *n*, *UCS*, and *SH*

Equation no.	Dependent variable	Estimator	Coefficient	R^2	*SEE*	F-ratio	Tabulated F-ratio
2	*CR* (m^2/h)	Constant *n* (%) *UCS* (MPa)	15.40 0.152 – 0.045	0.84	0.36	8.09	9.55
3	*CR* (m^2/h)	Constant *n* (%) *SH*	14.89 0.205 – 0.071	0.83	0.38	7.13	9.55
4	*CR* (m^2/h)	Constant *UCS* (MPa) *SH*	17.63 – 0.123 – 0.108	0.80	0.41	5.91	9.55

The analysis of variance (ANOVA) technique is used for testing the significance and global usefulness of multiple regression models. F statistics test is widely used in regression and

analysis of variance. The null hypothesis for this test is H_0: $\alpha_1 = \alpha_2 = 0$. Also, the alternative hypothesis is H_1: at least one of α_1 or α_2 is not equal to zero. Table 7 presents the ANOVA results for the regressions. For a significance level of 5%, the tabulated F-ratio with the degree of freedom $\upsilon_1 = 2$ and $\upsilon_2 = 3$ is 9.55. If the F-ratio is greater than the F-tabulated value obtained from the F distribution table; therefore, it can be said that the regression is significant (Stoodley et al., 1980). Since all of the F-ratios computed for the Eqs. (2-4) are quite larger than the tabulated F-ratios, the null hypothesis is rejected. Hence, it can be concluded that these equations are appropriate for estimating the *CR* of the samples using the *n*, *UCS*, and *SH* under the coefficients given in Table 7.

The estimation performance of a large-diameter circular saw plays a major role in decision-making for engineers. Besides, the sawability of building stones is the key factor in performance estimation. Instead of relying on only one method, using different approaches may improve the reliability of estimations and the confidence of the decision-makers. As stated by researchers, the models incorporating more variables are not useful due to their complexity and impracticality. Therefore, in this study, the practical equations based on these two variables are developed using multiple regression analyses.

The estimation capability of the simple and multiple equations was compared using the scatter diagrams of the estimated and measured *CR* values. The plots of estimated versus measured values of *CR* for simple and multiple equations are illustrated in Figs. 8 and 9, respectively. The error in the estimated value is represented by each data point's distance from the 1:1 diagonal line. A point on the line shows an accurate estimation. Since the points in Fig. 8 are scattered approximately uniformly around the diagonal line, it is inferred that the proposed simple regression equations are acceptable models for estimating the *CR* of the studied samples. However, for the multiple regression equations, the data points fall closer to the diagonal line and are lower scattered than those simple regression equations (Fig. 9). Comparison of R^2 of the simple and multiple equations and scatter diagrams exhibited the more accurate estimation performance of *CR* by multiple regression models than the simple regression models. Therefore, multiple regression equations are more appropriate and reliable than simple regression equations for estimating the *CR* of the samples.

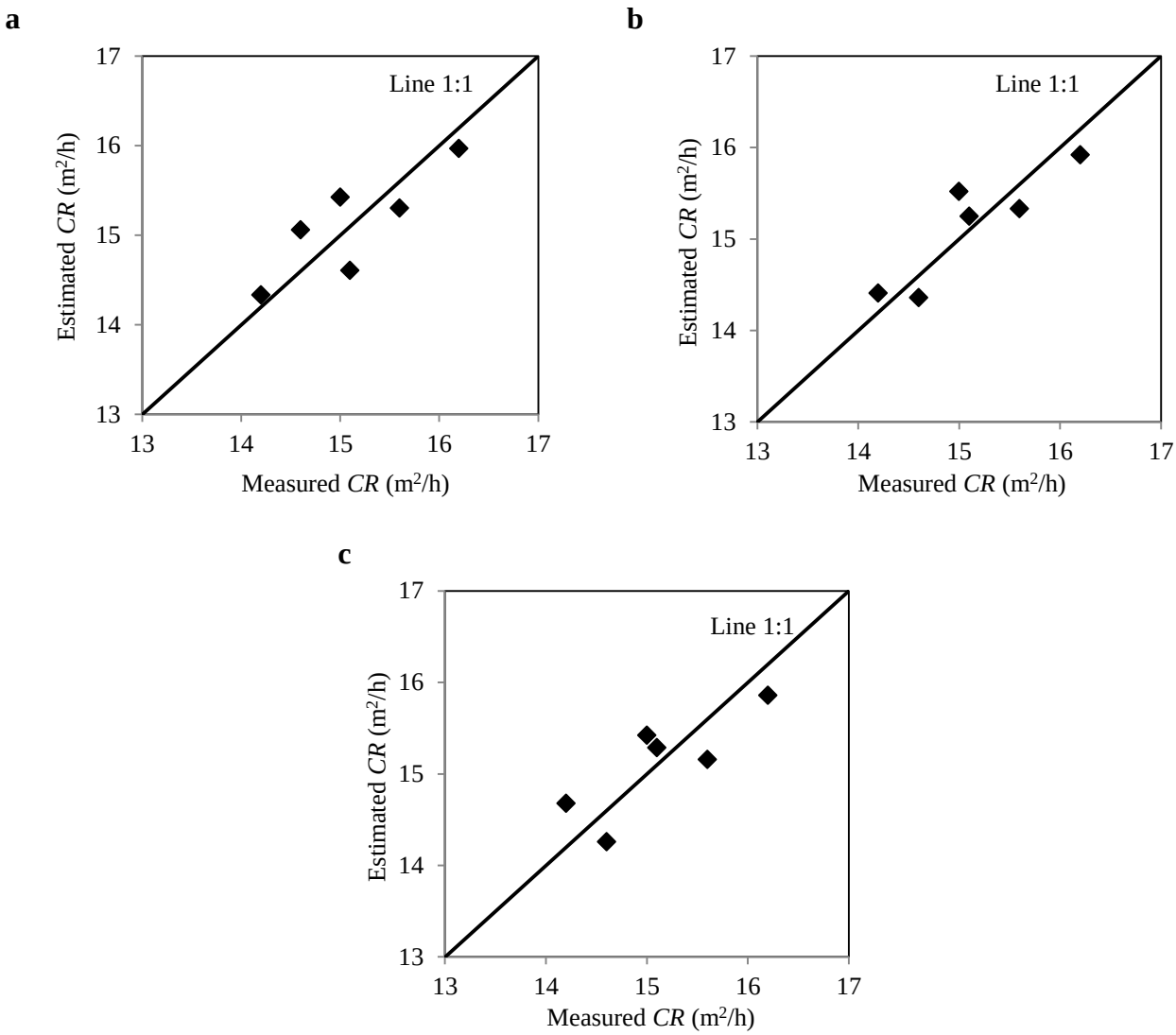

Figure 8. Measured *CR* versus *CR* estimated from simple regression equations (Fig. 7) based on **a)** *n*, **b)** *UCS*, and **c)** *SH*

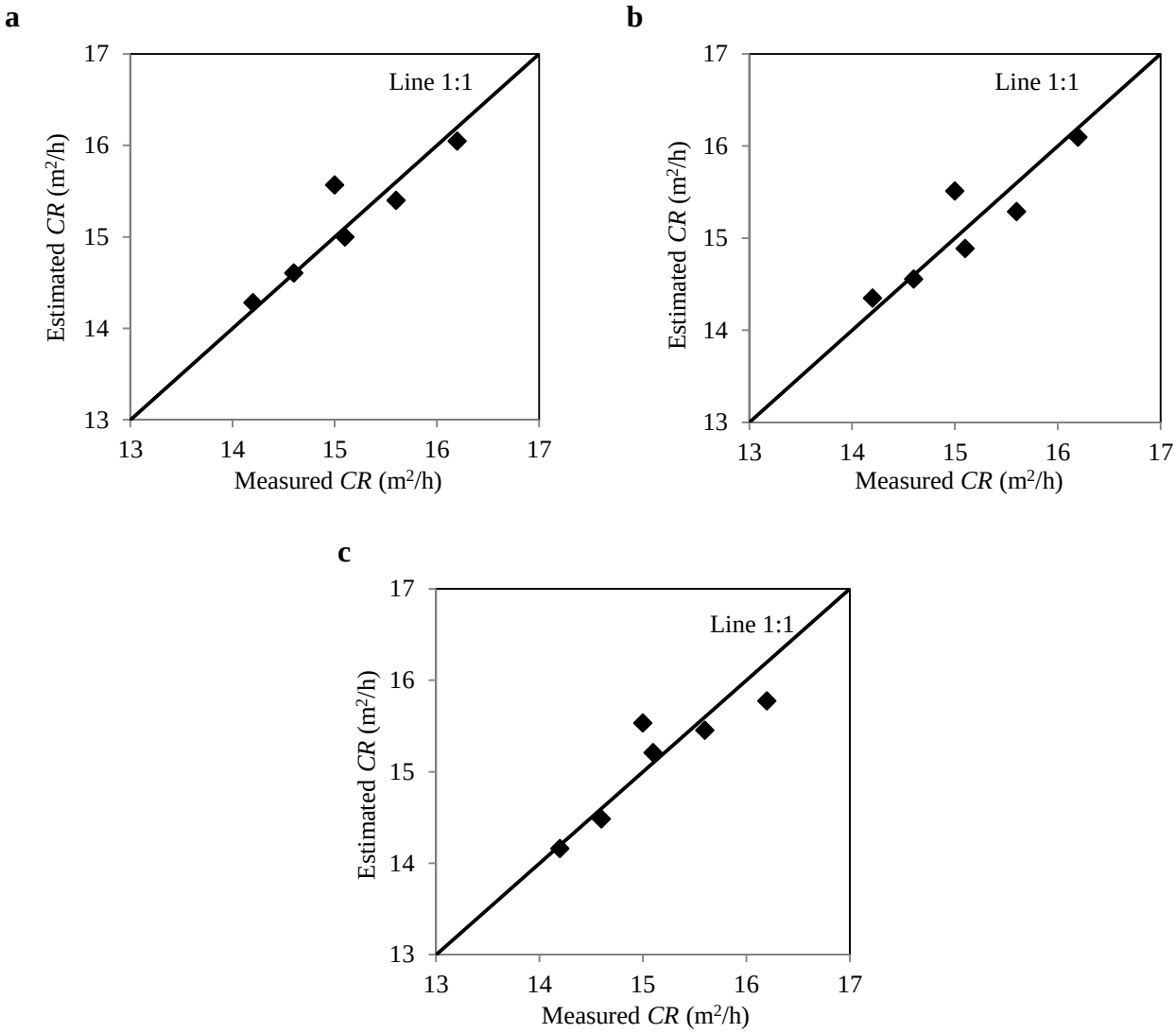

Figure 9. Measured *CR* versus *CR* estimated from multiple regression equations **a)** Eq. (2), **b)** Eq. (3), and **c)** Eq. (4)

Comparing the R^2 values of the simple and multiple equations and their 1:1 diagonal line reveals that Eq. (2) is the most accurate and reliable equation for estimating the *CR* of the samples. Thus, we only investigated the validity of Eq. (2), using the data from building stones published by Tumac (2016). This researcher studied the *CR* for some Turkish building stones such as limestone and marble from their *n* and *UCS* an. The measured values of these parameters in Tumac's (2016) research and those estimated from Eq. (2) are given in Table 8 and graphically illustrated in Fig. 10. According to this figure, the estimated *CR* from Eq. (2) is in fair agreement with the measured *CR* by Tumac (2016). This result reveals that the multiple regression model presented by Eq. (2) can be reliably used to estimate the building stones' *CR*. The slight difference in the measured values of *CR* in Tumac (2016) and those estimated from Eq. (7) is probably due to the difference in the stone type and physico-mechanical characteristics of the samples used.

Table 8. The measured *CR* from Tumac (2016) research and their *CR* from estimated Eq. (2) developed in this study

Rock type	Measured value			Estimated *CR* (m^2/h) value
	n **(%)**	***UCS*** **(MPa)**	***CR*** **(m^2/h)**	
Limestone 1	0.50	70.8	14.3	12.3
Limestone 1	0.30	89.0	12.4	11.4
Marble 1	0.27	81.3	11.3	11.8
Marble 2	0.40	65.3	15.4	12.5
Marble 3	0.20	70.4	16.3	12.3
Marble 4	0.11	63.8	11.9	12.5
Marble 5	0.09	70.2	13.4	12.3
Marble 6	0.2	77.8	12.3	11.9

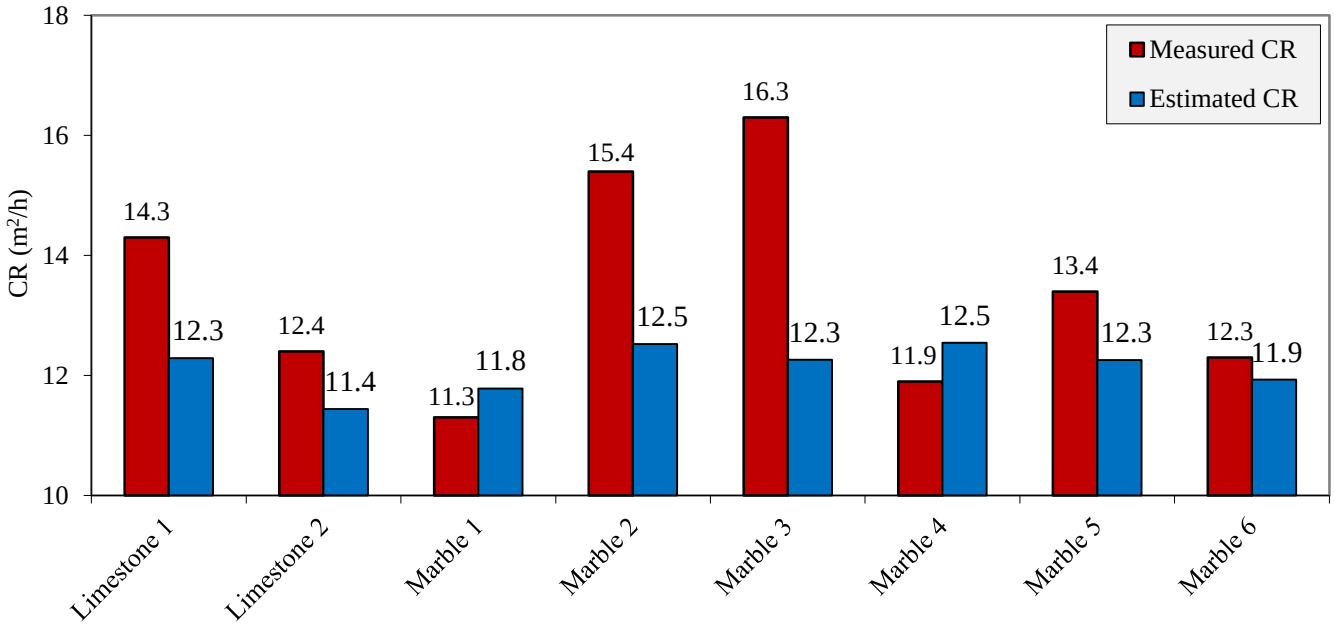

Figure 10. The measured *CR* by Tumac (2016) versus *CR* estimated from Eq. (2) developed in this study

5. Conclusions

The large-diameter circular saw is one of the most important machines used in stone processing plants. Performance estimation of the large-diameter circular saws is very important in the cost estimation of sawability and production planning of the stone processing plants. An accurate estimation of sawability helps make the planning of stone sawing projects more efficient. This study examined the relationships between *CR* with *n*, *UCS*, and *SH* for six different travertine samples using simple and multiple regression models.

The results of regression analyses revealed that the multiple regression models are more reliable than the simple regression models for estimating the *CR* of samples. The validity of multiple regression models was investigated using the raw data obtained from experimental works published by one researcher. The results revealed that multiple regression models accurately estimate the *CR* from *n* and *UCS*.

Finally, the developed multiple regression model in this study is helpful for stone engineers in processing factories of the building stones such that the performance of large-diameter saw machines can be estimated from *n* and *UCS* of the stone. Overall, the multiple regression models provide practical advantages for estimating *CR* and save much time and cost during the planning and design of the stone processing factories.

References

Almasi SN, Bagherpour R, Mikaeil R, Ozcelik Y, Kalhori H. Predicting the building stone cutting rate based on rock properties and device pullback amperage in quarries Using M5P model tree. Geotechnical and Geological Engineering 2017a;35:1311–1326.

Almasi SN, Bagherpour R, Mikaeil R, Ozcelik Y. Analysis of bead wear in diamond wire sawing considering the rock properties and production rate. Bulletin of Engineering Geology and the Environment 2017b;76:1593–1607.

Anon. Classification of rocks and soils for engineering geological mapping, part 1: Rock and soil materials. Bulletin Association Engineering Geology 1979;19:355–371.

Armaghani DJ, Mohamad ET, Hajihassani M, Yagiz S, Motaghedi H. Application of several non-linear prediction tools for estimating uniaxial compressive strength of granitic rocks and comparison of their performances. Engineering with Computers 2016;32:189–206.

Ataei M, Mikaiel R, Sereshki F, Ghaysari N. Predicting the production rate of diamond wire saw using statistical analysis. Arabian Journal of Geosciences 2012;5:1289–1295.

Aydin G, Karakurt I, Hamzacebi C. Performance prediction of diamond saw blades using artificial neural network and regression analysis. Arabian Journal for Science and Engineering 2015;40:2003–2012.

Bahrami S, Sarikhani R, Jamshidi A, Ghassemi Dehnavi A, Emami Mybodi MR. A comparative assessment of the effects of sodium and magnesium sulfates on the physico-mechanical characteristics of Abasabad Travertine, Mahallat, Urumieh-Dokhtar Magmatic Belt, Iran. Environmntal earth Sciences 2023;82:92.

Beiki M, Majdi A, Givshad AD. Application of genetic programming to predict the uniaxial compressive strength and elastic modulus of carbonate rocks. International Journal of Rock Mechanics and Mining Sciences 2013;63:159–169.

Burgess RB. Circular sawing granite with diamond saw blades. In: Proceedings of the fifth industrial diamond seminar 1978;3–10.

Ceryan N. Application of support vector machines and relevance vector machines in predicting uniaxial compressive strength of volcanic rocks. Journal of African Earth Sciences 2016;100:634–644.

Delgado NS, Rodriguez R, Rio A, Sarria ID, Calleja L, Argandona VGR. The influence of microhardness on the sawability of Pink Porrino granite (Spain). International Journal of Rock Mechanics and Mining Sciences 2005;42:161–166.

Fener M, Kahraman S, Ozder MO. Performance prediction of circular diamond saws from mechanical rock properties in cutting carbonate rocks. Rock Mechanics and Rock Engineering 2007;40: 505–517.

Gunaydin O, Kahraman S, Fener M. Sawability prediction of carbonate stones from brittleness indexes. Journal of the Southern African Institute of Mining and Metallurgy 2004;104:239–244.

Guney A. Performance prediction of large-diameter circular saws based on surface hardness tests for Mugla (Turkey) marbles. Rock Mechanics and Rock Engineering 2011;44:357–366.

ISRM. Rock characterization testing and monitoring. ISRM suggested methods. In: Brown ET (ed), 1981, Pergamon Press, Oxford.

ISRM. Suggested methods for determining hardness and abrasiveness of rocks. International Journal of Rock Mechanics and Mining Sciences 1978;15:89–98.

ISRM. The complete ISRM suggested methods for rock characterization, testing and monitoring. In: Ulusay R, Hudson JA (eds.), 2007, Suggested methods prepared by the commission on testing methods.

Jamshidi A, Nikudel MR, Khamehchiyan M, Zarei Sahamie R, Abdi Y. A correlation between P-wave velocity and Schmidt hardness with mechanical properties of travertine building stones. Arabian Journal of Geosciences 2016;9:568.

Jamshidi A. A new predictor parameter for production rate of ornamental stones. Bulletin of Engineering Geology and the Environment 2019;78:2565–2574.

Kahraman S, Altunb H, Tezekicib BS, Fener M. Sawability prediction of carbonate rocks from shear strength parameters using artificial neural networks. International Journal of Rock Mechanics and Mining Sciences 2006;43:157–164.

Kahraman S, Fener, M, Gunaydin O. Predicting the sawability of carbonate stones using multiple curvilinear regression analysis. International Journal of Rock Mechanics and Mining Sciences 2004;41:1123–1131.

Kahraman S, Gunaydin O. Indentation test to estimate the sawability of carbonate stones. Bulletin of Engineering Geology and the Environment 2008;67:507–511.

Madhubabu N, Singh P, Kainthola A, Mahanta B, Tripathy A, Singh T. Prediction of compressive strength and elastic modulus of carbonate rocks. Measurement 2016;88:202–213.

Mikaeil R, Ataei M, Yousefi R. Correlation of production rate of ornamental stone with rock brittleness indexes. Arabian Journal of Geosciences 2013a;6:115–121.

Mikaeil R, OzcelikY, Yousefi R, Ataei M, Hosseini SM. Ranking the sawability of ornamental stone using fuzzy Delphi and multi-criteria decision-making techniques. International Journal of Rock Mechanics and Mining Sciences 2013b;58:118–126.

Mishra D, Basu A. Estimation of uniaxial compressive strength of rock materials by index tests using regression analysis and fuzzy inference system. Engineering Geology 2013;160:54–68.

Mohamad ET, Armaghani DJ, Momeni E, Alavi Nezhad Khalil Abad V. Prediction of the unconfined compressive strength of soft rocks: a PSO-based ANN approach. Bulletin of Engineering Geology and the Environment 2015;74:745–757.

Pentecost A. Travertine. Springer, Berlin, 2005.

Rajpurohit SS, Sinha RS, Sen P. Influence of Cerchar hardness index of hard rock granite on wear of diamond tools. Materials Today: Proceedings, 2020.

Roshanak R, Moore F, Zarasvandi AR, Keshavarzi B, Gratzer R. Stable isotope geochemistry and petrography of the Qorveh-Takab travertines in northwest Iran. Austrian Journal of Earth Sciences 2018;111:64–74.

Singh P, Tripathy A, Kainthola A, Mahanta B, Singh V, Singh T. Indirect estimation of compressive and shear strength from simple index tests. Engineering with Computers 2017;33:1–11.

Stoodley KDC, Lewis T, Stainton CLS. Applied statistical techniques. England: Ellis Horwood, 1980.

Tumac D. Artificial neural network application to predict the sawability performance of large diameter circular saws. Measurement 2016;80:12–20.

Tumac D. Predicting the performance of large diameter circular saws based on Schmidt hammer and other properties for some Turkish carbonate stones. International Journal of Rock Mechanics and Mining Sciences 2015;75:159–168.

Yurdakul M, Gopalakrishnan K, Akdas H. Prediction of specific cutting energy in natural stone cutting processes using the neuro-fuzzy methodology. International Journal of Rock Mechanics and Mining Sciences 2014;67:127–135.

Zalooli A, Khamehchiyan M, Nikudel MR. The quantification of total and effective porosities in travertines using PIA and saturation-buoyancy methods and the implication for strength and durability. Bulletin of Engineering Geology and the Environment 2018;77:1739–1751.

Zarasvandi A, Roshanak R, Gratzer R, Pourkaseb H, Moore F. Stable isotope geochemistry of travertines from northern Urumieh-Dokhtar volcano-plutonic belt, Iran. Carbonates and Evaporites 2019;34:869–881.